Solution Properties of Polyisobutylene Investigated by Using Dynamic and Static Light Scattering and Pulsed Field Gradient NMR

Wyn Brown* and Pu Zhou

Institute of Physical Chemistry, Box 532, 751 21 Uppsala, Sweden

Received November 27, 1990; Revised Manuscript Received April 4, 1991

ABSTRACT: The solution properties of the flexible polymer polyisobutylene (PIB) with chloroform as solvent are compared with those of polystyrene (PS) in good solvents over a broad concentration range extending from dilute through the semidilute regime. The methods included both static and dynamic light scattering, and frictional coefficients were evaluated by using pulsed field gradient NMR. The latter technique was also used to obtain self-diffusion coefficients for PIB in the Θ solvent benzene (24.5 °C), which is isorefractive with PIB. The "universal" ratio $\rho = R_g/R_h$ is unusually large ($\rho \approx 1.77$) compared with the value for PS in good solvents (≈1.5), showing a possible difference in draining behavior. In semidilute solution, the dynamic length scales for PS and PIB are identical at the same weight concentration even though the different entanglement densities might have been expected to make themselves felt. Small systematic deviations from the behavior predicted by renormalization group theory exist and are similar for both types of chain.

Introduction

Polystyrene is traditionally the polymer of choice for investigations of solution properties (dilute and semidilute) owing to the general availability of fractions of narrow molecular weight distribution, extending over wide ranges of molecular weight. It is important, however, when experimental results are compared with predictions of theory to include data for other polymer types differing in backbone structure since chain flexibility may play an important role, particularly with the dynamic quantities which are sensitive to temporary entanglements.

Extensive studies of the properties of polyisobutylene (PIB) have been made in this laboratory to some extent to fill this need. PIB fractions have, for example, been used as a semidilute matrix in ternary systems for investigation of the transport of hard spheres in PIB solutions,[1] with PIB chains of both high and low molecular weight as probes in the homopolymeric systems,[2,3] and also in conjunction with polystyrene chains[4] to study the effects of mutual chain incompatibility on transport processes.

The present paper assembles parameters, on the one hand, for dilute solutions of PIB in chloroform, the data mainly being evaluated in terms of renormalization group (RG) expressions[5] and, on the other, for the semidilute concentration range with similar comparisons made with theoretical predictions. The behavior of polystyrene in semidilute solutions has recently been reviewed,[6] and these collected data serve as a reference frame for comparisons between the two polymers.

The experimental methods employed are mainly static (SLS) and dynamic light scattering (DLS), pulsed field gradient NMR (PFG NMR), and viscosity. NMR was also used to obtain self-diffusion coefficients in the Θ solvent benzene (24.5 °C) in which system light scattering could not be made since the refractive indices of polymer and solvent are closely similar. The NMR data are important for two reasons: (a) they give directly the friction coefficient in dilute solution, and (b) combination of dynamic light scattering mutual diffusion and NMR self-diffusion coefficients allows evaluation of the inverse osmotic compressibility.

Experimental Section

Polyisobutylenes (PIB) were from Polymer Standards Service, Mainz, FRG, the characteristics of which have been given previously.[1] These fractions have a low but not insignificant polydispersity since M_w/M_n is approximately 1.2, independent of molecular weight. Samples of molecular weight greater than 1.1×10^6 were kindly supplied by BASF, Ludwigshafen, FRG. These samples were characterized by using static light scattering, but the M_w/M_n ratio is not known. Solutions were filtered by using Millipore (fluoropore) 0.22-μm filters directly into 10-mm precision bore NMR tubes of high quality. The tubes were capped by using similar filters and the higher concentrations prepared by very slow evaporation of the solvent (chloroform) at low temperature. Approximately 4 months was required to prepare the range of concentrations used in the DLS measurements at semidilute concentrations.

Intensity light scattering measurements were made by using a photon-counting apparatus supplied by Hamamatsu to register the scattered signal. The light source was a 3-mW He–Ne laser. The optical constant for vertically polarized light is $K = 4\pi^2 n_0^2 (dn/dc)^2/N_A\lambda^4$, where n_0 is the solvent refractive index, dn/dc the measured refractive index increment in chloroform (=0.075 mL g^{-1} at 25 °C), and λ the wavelength (633 nm). We note that the previously reported[1] value of dn/dc (=0.095 mL g^{-1}) was erroneously high. The reduced scattered intensity, KC/R_θ was derived, where C is the concentration and R_θ is the Rayleigh ratio obtained through calibration using benzene; $R_{90} = 8.51 \times 10^{-6}$.[7] The angle-corrected intensity for benzene was determined over the angular range 30–160 °C, and these values were used in the calculation of the Rayleigh ratio of the PIB solution at each angle. Precise measurements of the angular dependence of KC/R_θ could be made for the different fractions and gave the radius of gyration, R_g, from the slopes of the $C = 0$ line divided by the intercept ($=1/M_w$). The second virial coefficients were obtained from the slope of the zero-angle plots.

Table II summarizes the data obtained from the intensity light scattering measurements. The radii of gyration given here are lower than those previously reported due to the above-mentioned redetermination of dn/dc. The values of the inverse osmotic compressibility ($\partial\pi/\partial C$) were evaluated from the values of KC/R_θ.

Dynamic light scattering measurements have been made by using the apparatus and technique described in ref 8. Laplace inversion of the correlation curves was performed by using a constrained regularization program REPES[9] to obtain the distribution of decay times. The algorithm differs in a major respect from CONTIN in that the program directly minimizes the sum of the squared differences between the experimental and calculated $g_2(t)$ functions using nonlinear programming, and the

0024-9297/91/2224-5151$02.50/0

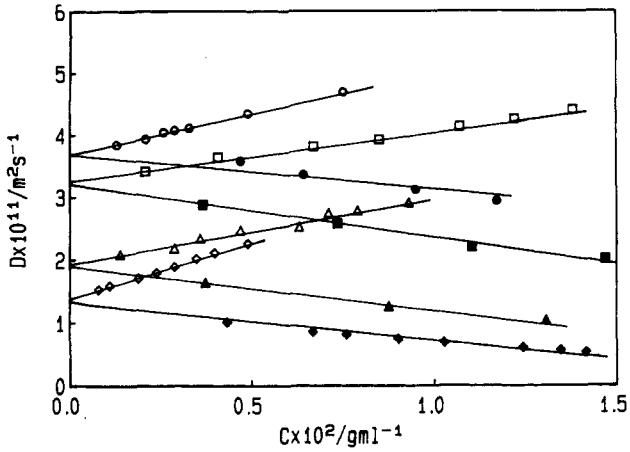

Figure 1. Diffusion coefficients for PIB in chloroform obtained by dynamic light scattering (open points) and pulsed field gradient NMR (solid points): 1.82×10^5 (circles); 2.47×10^5 (squares); 6.1×10^5 (triangles); 1.1×10^6 (diamonds).

a priori chosen parameter "probability to reject" was selected as $P = 0.5$. Decay time distributions determined by using this inversion program are similar to those obtained by using CONTIN with a similar degree of smoothing. In the present case, the correlation functions were close to single exponentials and the decay time distributions single-peaked. The relaxation rates gave values close to those determined by using a second-order cumulants fit. The measurements were performed at low angle ($\theta < 60°$) such that contributions from internal modes could be neglected. It was established that (Γ/q^2) was independent of angle.

Pulsed field gradient NMR measurements were made on protons at 99.6 MHz on a standard JEOL FX-100 Fourier transform NMR spectrometer as previously described.[10] An internal deuterium lock ($CDCl_3$; C_6D_6) was used for field frequency stabilization.

Due to the favorably long transverse relaxation time (T_2) the field gradient pulses could be spaced as widely as 240 ms, thus allowing longer durations of the gradient pulses. The lower range of accessible diffusion coefficients lay between 10^{-11} and 10^{-12} m^2 s^{-1}. The experimental uncertainty is about ±1.5% at a value of $D^* = 10^{-11}$ m^2 s^{-1}.

Intrinsic viscosity measurements were made at 25 °C by using an Ubbelohde capillary viscometer. Shear dependence corrections were not made.

Partial specific volume measurements were made by using a digital density instrument (DMA 60, Anton Paar, Graz, Austria) at 25 °C for solutions up to 5% (w/w). The volume (V) of solution containing 1 kg of solvent was calculated from the measured density of solution, the concentration of which was expressed as kilograms of PIB per kilogram of $CHCl_3$. V was plotted against the latter and the partial specific volume (v_2) obtained as the slope of the curve. The value was found to be 1.069 ± 0.002 mL g^{-1}.

Results

Figure 1 shows typical diffusion coefficient data for four fractions of PIB in $CHCl_3$ at dilute concentrations obtained by using DLS and PFG NMR. The common intercept at infinite dilution gives D_0.

Log–log plots of D_0 vs molecular weight for all fractions used in chloroform and benzene are given in Figure 2. The equation of the line in chloroform is

$$(D_0)_z = 6.22 \times 10^{-8} M^{-0.60} \text{ m}^2 \text{ s}^{-1} \quad (1a)$$

The corresponding relationship in benzene at 24.5 °C (θ conditions) is

$$(D_0)_z = 1.27 \times 10^{-8} M^{-0.48} \text{ m}^2 \text{ s}^{-1} \quad (1b)$$

The concentration dependence of the mutual diffusion

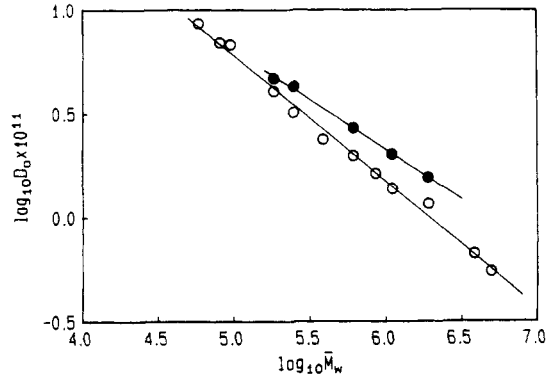

Figure 2. Diffusion coefficients at infinite dilution $(D_0)_z$ as a function of molecular weight for PIB in chloroform (open points) and benzene (solid points). The equations of the lines are given in eqs 1a and 1b.

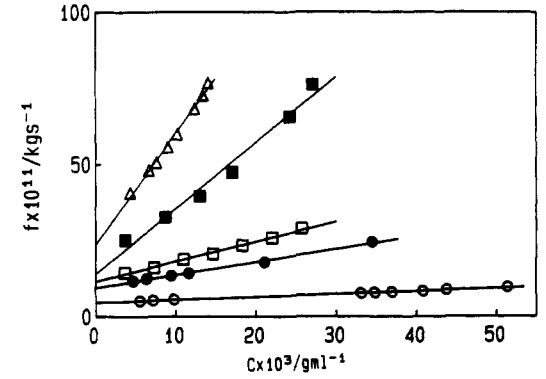

Figure 3. Friction coefficients $f = (kT/D^*)$ calculated from pulsed field gradient NMR diffusion coefficients (D^*) shown as a function of concentration for PIB in chlorform: $M = 5.71 \times 10^4$ (○), 1.82×10^5 (●), 2.47×10^5 (□), 6.1×10^5 (■), 1.1×10^6 (△).

coefficient at finite concentration is given by[11]

$$D = (kT/f)_c(1 - \Phi)(1 + 2A_2MC + ...) \quad (2)$$

where Φ is the polymer volume fraction and A_2 the second virial coefficient. $(kT/f)_c$ is the self-diffusion coefficient (D^*), with f the strongly concentration dependent friction coefficient at concentration C. Figure 3 shows the concentration dependence of f for selected fractions, where these data were obtained from D^* measured by PFG NMR. This technique inherently monitors purely geometric lateral displacements of individual chains during a time typically of the order 10–2000 ms (here 240 ms) and which corresponds to a distance of 40–50 coil diameters. The coefficients k_f in the concentration expansion for the friction factor

$$f = f_0(1 + k_fC) \quad (3)$$

are plotted in Figure 4 as a function of molecular weight in a log–log diagram. The following relationship applies:

$$k_f = 1.83 \times 10^{-3} M^{0.85} \text{ mL g}^{-1} \quad (4)$$

In the dilute range, the concentration dependence of the translational diffusion coefficient may be approximated by

$$(D)_{25} = D_0(1 + k_DC + ...) \quad (5)$$

The molecular weight dependence of k_D is shown in Figure 5 and corresponds to

$$k_D = 1.92 \times 10^{-2} M^{0.66} \text{ mL g}^{-1} \quad (6)$$

In terms of A_2, one may write for the interrelationship

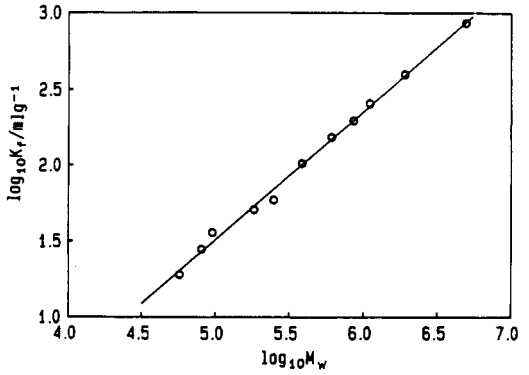

Figure 4. Slopes in Figure 3 according to $f = f_0(1 + k_fC)$ shown as a function of molecular weight for PIB in chloroform (eq 4).

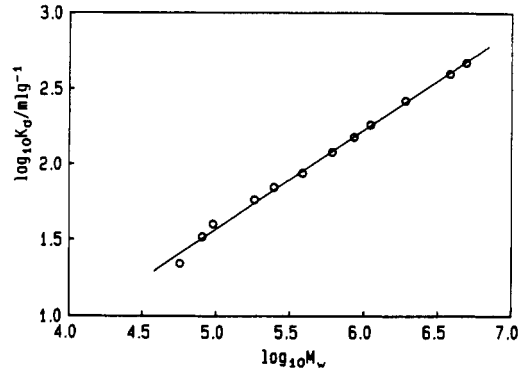

Figure 5. Slopes (k_D) according to $D = D_0(1 + k_DC + ...)$ as a function of molecular weight for PIB in chloroform (eq 6).

Table I
Hydrodynamic Parameters for PIB in Chloroform (25 °C)[a]

$M_w \times 10^{-3}$	$D_0 \times 10^{11}$, $m^2\ s^{-1}$	k_D, mL g^{-1}	k_f, mL g^{-1}	$(k_D)_{calc}$, mL g^{-1}	R_h, Å	$[\eta]$, mL g^{-1}	R_η, Å	R_η/R_h
57.1	8.56	22	19	21	45	29.3	65	1.35
80.4	6.94	33	28	27	60	35.3	75	1.35
95.0	6.79	40	36	28	60	38.8	85	1.40
182	4.02	58	51	53	100	55.4	115	1.15
247	3.19	70	59	76	125	65.7	125	1.0
385	2.36	87	103	85	170	83.7	170	1.0
610	1.97	120	154	124	205	107.9	220	1.05
856	1.62	151	198	167	250	130.0	260	1.05
1100	1.37	182	256	187	295	149.2	295	1.0
1900	1.24	263	397	294	325	201.9	395	1.2
3800	0.67	398	736	456	605	295.0	560	0.95
4900	0.55	472	855	594	730	338.5	640	0.90

[a] $(k_D)_{calc}$ from $k_D = 2A_2M - k_f - v_2$ (ref 11) ($v_2 = 1.069$). $R_\eta = (3M[\eta]/2.5N_A4\pi)^{1/3}$. R_h from Stokes–Einstein equation. k_f from pulsed field gradient NMR. k_D from DLS.

between k_D and k_f[11]

$$k_D = 2A_2M - k_f - v_2 \tag{7}$$

where v_2 is the partial specific volume.

k_D may be estimated by employing values of A_2 from SLS measurements (Figure 8) and the value $v_2 = 1.069$ mL g^{-1} determined by density measurements (Experimental Section). These values are given in Table I and are in excellent agreement with those from experiment. Values of the hydrodynamic radius (R_h) calculated from the D_0 values using the Stokes–Einstein relationship ($R_h = kT/6\pi\eta_0D_0$, where η_0 is the solvent viscosity) are included in Table I.

Intrinsic viscosities, $[\eta]$, are included in Table I for PIB in $CHCl_3$ and also in the Θ solvent benzene (24.5 °C) in Table III. We use the definition $C^* = 3M/4\pi R_g^3N_A$ and note that $C^* \approx 1/[\eta]$.[12] Relationships between the intrinsic

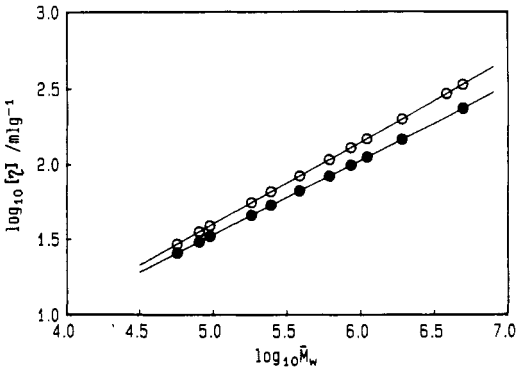

Figure 6. Intrinsic viscosities ($[\eta]$) for PIB in chloroform (open points) and benzene (solid points) as functions of molecular weight (eqs 8a and 8b).

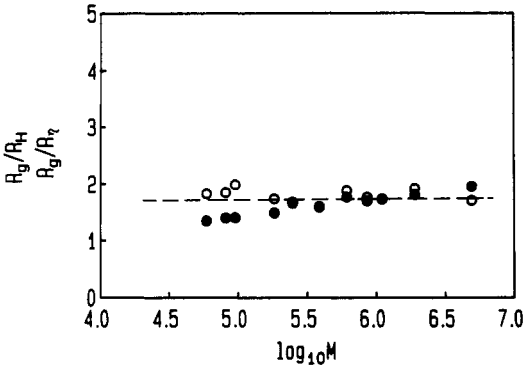

Figure 7. Ratio of the radius of gyration and hydrodynamic radius from diffusion coefficients (open points) and hydrodynamic radius from intrinsic viscosity (solid points). Data are for PIB in chloroform at 25 °C.

viscosity and molecular weight are shown in Figure 6. The equations of the lines are

$$[\eta]_{25} = 7.1 \times 10^{-2}M^{0.55\pm0.02}\ \text{(chloroform) mL g}^{-1} \tag{8a}$$

$$[\eta]_{24.5} = 0.11 \times M^{0.5\pm0.02}\ \text{(benzene) mL g}^{-1} \tag{8b}$$

This exponent in $CHCl_3$ is more in keeping with the value anticipated in a marginal solvent, whereas the exponents determined for the static and dynamic radii (eqs 13, 14a) suggest that $CHCl_3$ is a good solvent for PIB. One possibility, which would result in a low molecular weight exponent, is that there is a significant shear dependence of the intrinsic viscosity for the highest molecular weights. The small trend in the ratio (R_g/R_η), where R_η is the radius from the intrinsic viscosity (eq 9) seen in Figure 7, could support this as a contributory factor. It is not anticipated that polydispersity effects would lead to such a discrepancy in the molecular weight exponents since the polydispersity ratios are low ($M_w/M_n \approx 1.2$).

The hydrodynamic radii (R_η) (giving the solid points in Figure 7) have been calculated (Table I) as the hard-sphere radius from the hydrodynamic volume obtained from the intrinsic viscosity, V_h, by using the relationship

$$V_h = M[\eta]/2.5N_A \quad \text{with } V_h = (4/3)\pi R_\eta^3 \tag{9}$$

Within experimental uncertainty, the hydrodynamic radii as a function of molecular weight derived from the two sets of data agree, the average value of R_η/R_h being 1.03. There is considerable scatter, and the ratio at low molecular weights is significantly larger than at higher molecular weights. Since R_η should be the most precise

Table II
Parameters from Intensity Light Scattering for PIB in Chloroform

$M_w \times 10^{-3}$	R_g, Å	$A_2 \times 10^4$, cm^3 mol g^{-2}	R_{A_2},[a] Å	R_{A_2}/R_h[b]
57.1	85	3.63	50	1.05
80.4	105	3.47	60	1.05
95	115	3.41	65	1.15
182	175	2.88	100	1.0
247	208	2.75	120	0.95
385	270	2.46	155	0.9
610	360	2.29	205	1.0
856	440	2.14	250	1.0
1100	510	2.02	290	1.0
1900	710	1.82	400	1.25
3800	1075	1.57	610	1.0
4900	1250	1.48	705	0.95

[a] $R_{A_2} = (3M^2A_2/16\pi N_A)^{1/3}$ (ref 11). [b] R_h from Table III.

Table III
Hydrodynamic Parameters for PIB in Benzene (24.5 °C; θ Conditions)

$M_w \times 10^{-3}$	k_f, mL g^{-1}	$D_0 \times 10^{11}$, m^2 s^{-1}	R_h, Å	$[\eta]$, mL g^{-1}	R_η, Å	R_η/R_h
57.1				25.5		
80.4				30.3		
95.0				33.0		
182	31	3.69	95	45.6	110	1.15
247	38	3.37	105	53.3	130	1.2
385				66.4	160	
610	112	2.13	170	83.5	200	1.2
856				99.0	240	
1100	198	1.59	225	112.2	270	1.2
1900	312	1.23	290	147.7	355	1.2
4900				236.3	570	

dimension, the scatter must derive from uncertainty in the D_0 values for the low molecular weights. The ratio R_η/R_h is predicted by RG theory[13] to be approximately 1.1 but, here again, experiment shows considerable differences depending on the solvent (draining character). The exponent of 0.5 in eq 8b is that anticipated for Θ conditions.

Static light scattering data in chloroform are summarized in Table II. The molecular weight dependence of A_2 (Figure 8) is given by

$$A_2 = 3.45 \times 10^{-3} M^{-0.204} \quad (10)$$

An exponent of −0.20 is expected in good solvents using the hard-sphere approximation.[11] Second virial coefficients were also determined from the diffusion coefficients measured by DLS (D) and PFG NMR (D^*) using the relationship

$$(D/D^*) = (M/RT)(\partial\pi/\partial C)_{T,P} = (1 + 2A_2MC + ...) \quad (11)$$

The agreement between the A_2 values and those from static light scattering is excellent as shown in Figure 8.

An apparent radius may also be calculated from the second virial coefficient:

$$R_{A_2} = (3M^2A_2/16\pi N_A)^{1/3} \quad (12)$$

These values are given in Table II. As pointed out by Akcasu,[33] R_{A_2} corresponds to the effective radius of interaction, and in a good solvent this should coincide with the hard-sphere radius.

The average value of the ratio R_{A_2}/R_h is 1.02. The latter will vary from zero at the Θ temperature to about unity in the good solvent limit.

The radius of gyration (Table II) should scale with molecular weight as $R_g \sim M^{0.5}$ in Θ solvents and the exponent

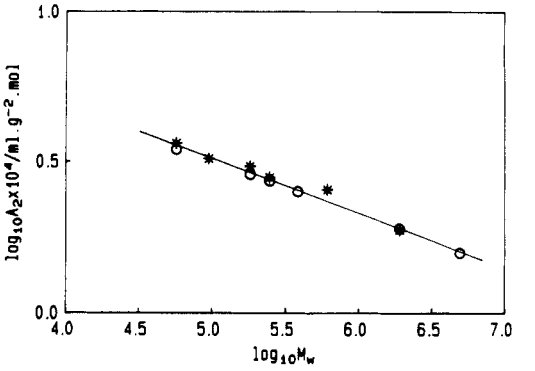

Figure 8. Molecular weight dependence of the second virial coefficient from static light scattering (○) and the ratio (D/D^*) according to eq 11 (*). See eq 10.

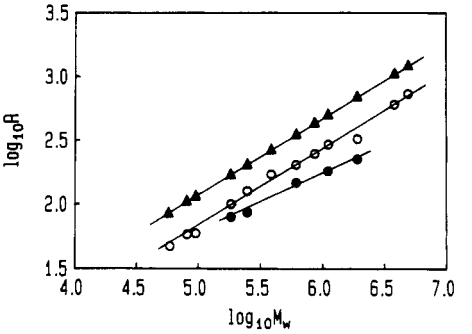

Figure 9. Radii of gyration and hydrodynamic radii (R_h) as a function of molecular weight: R_g chloroform (▲); R_h chloroform (○); R_h benzene (●).

(ν) should increase to a limiting value of 0.588 in very good solvents according to RG theory. In the PIB/$CHCl_3$ system, the radius of gyration (R_g) values are shown as a function of M in Figure 9 and correspond to

$$(R_g)_z = 0.121M^{0.60\pm0.03} \text{ Å} \quad (13)$$

Included in Figure 9 are values of the hydrodynamic radius (R_h) giving the corresponding relationship:

$$R_h = 6.4 \times 10^{-2} M^{0.60\pm0.02} \text{ (chloroform) Å} \quad (14a)$$

In benzene we obtain

$$R_h = 0.28M^{0.47\pm0.03} \quad (14b)$$

which is approximately the value anticipated (0.5) in a Θ solvent.

Discussion

Dilute Solutions. The dimensionless ratio

$$\rho = R_g/R_h \quad (15)$$

where R_h is defined as the hydrodynamic radius obtained by using the Stokes–Einstein equation, has been suggested as a sensitive index of the particle conformation. For hard spheres ρ = 0.778. For coils under Θ conditions, ρ has been considered to take a universal value of approximately 1.50, although this conclusion conflicts with experiment. Thus, Schmidt and Burchard[14] report ρ = 1.27 for PS in a variety of Θ systems, a value which agrees with calculations by Zimm[15] for nondraining Gaussian coils in the absence of hydrodynamic screening. In good solvent systems, on the other hand, the experimental value for PS is frequently found to lie in the region of 1.5, in agreement with RG calculations for nondraining chains.[16-18] Thus,

Table IV
Comparison of Dilute Solution Parameters for Various Polymers at a Chain Length P_w = 17 860 (M_{PIB} = 1 × 10⁶)[a]

	PIP	PS	PIB	PNiPMAM	PNiPAM
R_g, Å	695	650	480	774	566
R_h, Å	465	449	255	449	404
R_{Flory},[b] Å	569	583	340	505	464
$D_0 \times 10^7$, cm² s⁻¹	0.52	0.88	1.56	0.48	0.61
$A_2 \times 10^4$, mol cm³ g⁻¹	5.95	2.67	2.0	1.51	1.4
$[\eta]$, cm³ g⁻¹	558	392	142	205	183
$\rho = R_g/R_h$	1.49	1.45	1.77	1.72	1.4
$(R_g^0)^2/P_w \times 10^{15}$, Å²	0.76	0.87	1.05	2.2	1.1

PIP/cyclohexane (ref 34)	PS/benzene (refs 35, 36)
$R_g = 0.135M^{0.61}$	$R_g = 0.1212M^{0.595}$
$R_h = 9.03 \times 10^{-2}M^{0.61}$	$R_h = 0.16M^{0.55}$
$R^0_g = 3.35 \times 10^{-9}M^{0.50}$	$R^0_g = 0.29M^{0.50}$
$A_2 = 9.8 \times 10^{-3}M^{-0.20}$	$A_2 = 1.17 \times 10^{-2}M^{-0.262}$
$D_0 = 2.69 \times 10^{-4}M^{-0.61}$	$D_0 = 2.46 \times 10^{-4}M^{0.55}$
$[\eta] = 1.59 \times 10^{-2}M^{0.747}$	$[\eta] = 7.8 \times 10^{-3}M^{0.75}$

PIB/$CHCl_3$ (this work)	PNiPMAM/water (ref 38b)	PNiPAM/water (ref 38a)
$R_g = 0.121M^{0.60}$	$R_g = 0.158M^{0.58}$	$R_g = 0.0224M^{0.54}$
$R_h = 6.4 \times 10^{-2}M^{0.60}$	$R_h = 0.106M^{0.57}$	$R_h = 0.016M^{0.54}$
$A_2 = 3.45 \times 10^{-3}M^{-0.204}$	$A_2 = 5.9 \times 10^{-3}M^{-0.25}$	$A_2 = M^{-0.34}$
$D_0 = 6.22 \times 10^{-4}M^{0.60}$	$D_0 = 2.02 \times 10^{-4}M^{-0.57}$	$D_0 = M^{-0.54}$
$[\eta] = 7.1 \times 10^{-2}M^{0.55}$	$[\eta] = 9.66 \times 10^{-3}M^{0.68}$	$[\eta] = 0.112M^{0.51}$

[a] PIP, polyisoprene; PS, polystyrene; PIB, polyisobutylene; PNiPMAM, poly(*N*-isopropylmethacrylamide); PNiPAM, poly(*N*-isopropylacrylamide). [b] R_{Flory} was calculated from $[\eta]$ by using the Flory–Fox equation.

there would appear to be a consensus indicating a systematic increase in ρ with increasing solvent quality as well as a strong influence of the polydispersity.

Akcasu et al.[37] also predict that ρ should depend on solvent quality, the values ranging from 1.5 under Θ conditions to 1.86 in a good solvent.

Bhatt and Jamieson,[18] however, report very different values for polystyrene in good solvents: 1.57 (ethylbenzene) and 1.3 (THF). Although the radii of gyration were found to be the same in these media, the second virial coefficients and hydrodynamic radii are larger in THF, indicating that the draining effects in these solvents differ, i.e., that the internal hydrodynamic interactions may be nonuniversal. Supporting this, Douglas and Freed[19] recently concluded from RG calculations that ρ is independent of solvent quality and varies only with hydrodynamic draining character. In the present case we find an average value of ρ = 1.77 (Figure 7) in the asymptotic limit of high molecular weight. Since the PIB chains are not very polydisperse, the source of the difference between this value and that for PS (1.51; ref 6) could lie in differences in draining characteristics: the PIB chain may be less solvated and the draining effects larger than in PS.

Table IV summarizes some dilute solution parameters for different polymer/solvent systems including PIB. To facilitate comparison, the various parameters have been calculated at a common weight-average degree of polymerization of 17 860 (which corresponds to an arbitrarily chosen molecular weight for PIB of $M = 1 \times 10^6$). The unusual polymers poly(*N*-isopropylacrylamide) (PNiPAM; ref 38a) and poly(*N*-isopropylmethacrylamide) (PNiPMAM; ref 38b) in water are also included since the latter displays an unusual degree of chain stiffness. With PIB, R_h and the Flory–Fox radius are substantially smaller than the radius of gyration, as illustrated by the tabulated values of ρ. The unperturbed dimensions ($(R_g^0)^2/P_w$) for PIB and PNiPMAM also substantially exceed those for PIP and PS and reflect higher degrees of chain stiffness in the

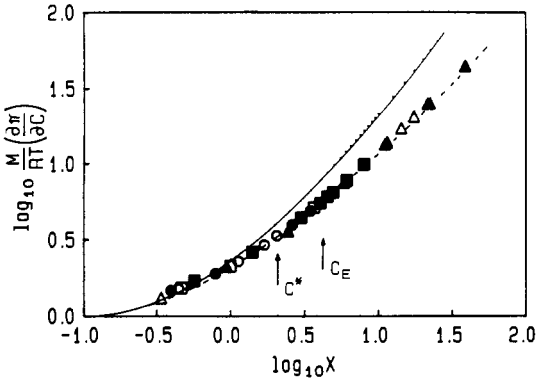

Figure 10. Reduced osmotic compressibility vs the excluded volume parameter X (ref 5) for PIB in chloroform at 25 °C. The continuous line has been obtained from theory from which, to a first approximation, $X = (16/9)A_2MC$. Approximate positions of the overlap parameter (C^*) and the entanglement concentration (C_E; note 31) are shown. $M = 5.7 \times 10^4$ (○), 1.82×10^5 (●), 2.47×10^5 (□), 3.85×10^5 (■), 1.9×10^6 (△), 4.9×10^6 (▲).

former (R_g^0 has been calculated for PIB by using the expansion factor calculated with eq 21). It is particularly interesting from the point of view of the PIB structure which has two pendant methyl groups on each monomer to note the effect on the radius of gyration and the unperturbed dimensions of the extra methyl group in PNiPMAM in comparison with PNiPAM, although this is possibly mostly associated with a change in solvation structure in the aqueous system. The large variations in behavior displayed in Table IV appear to support the conclusions of Jamieson and co-workers on the important part played by differences in draining properties and the lack of universality.

Application of Renormalization Group (RG) Theory. Static Properties: Inverse Osmotic Compressibility. Renormalization group theory predicts universal characteristics of polymer systems with excluded volume effects. One such universal function is the dimensionless, static parameter: $(M/RT)(\partial\pi/\partial C)$. Ohta and Oona[21,22] have given an expression for this function in terms of the dimensionless parameter X which is uniquely related to the second virial coefficient and to a first approximation given by

$$X = (16/9)A_2MC \tag{16}$$

Such a plot is shown in Figure 10 with the continuous line representing the theoretical prediction. The data indeed support the supposition of a universal function, at least up to $18C^*$. However, with PIB the divergence is in the opposite sense to that observed by a number of other authors, for example, for polystyrene/toluene[23] and for poly(ethylene oxide)/methanol.[24] A similar discrepancy is found for the hydrodynamic quantity (see below).

The Virial Coefficient–Coil Interpenetration Function. Available theories predict that the interpenetration function (Ψ) should be a universal function of the radius expansion factor α, where

$$\Psi = A_2M^2/4\pi^{3/2}N_AR_g^3 \tag{17}$$

Experimental data for the second virial coefficient may thus be expressed in terms of Ψ which is related to the draining behavior. Values of the interpenetration function are shown in Figure 11 plotted against the expansion factor evaluated from viscosity data according to eq 21. The asymptotic value for the present data lies in the region of 0.23, indicating that chloroform is a good solvent for PIB. This conclusion is consistent with the exponent in $R_g \sim$

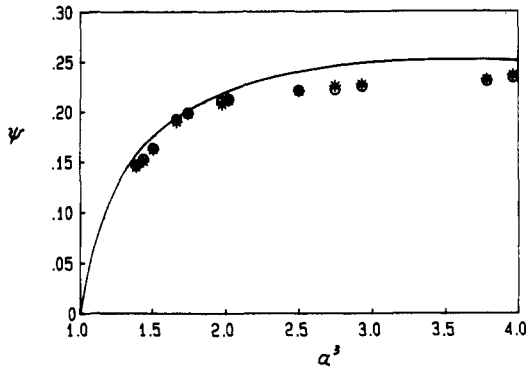

Figure 11. Penetration parameter (Ψ) (eq 17) shown as a function of the expansion parameter (α_η^3) for PIB in chloroform at 25 °C: using A_2 values (*); using k_f values (○). The solid curve was estimated according to eqs 17–20.

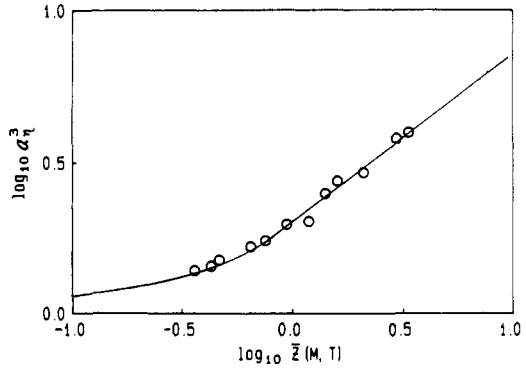

Figure 12. Change in the viscosimetric expansion factor with the z parameter. The solid line is plotted according to eq 22.

M^ν and that for the molecular weight dependence of the diffusion coefficient. Theory[25] predicts a monotonic increase in Ψ with increasing solvent quality (the parameter Z or the expansion factor α) and should reach a constant asymptotic value of $\Psi = 0.269$ for very good solvents. The solid curve from RG theory was calculated by using the following parameter-free prediction:[5]

$$\Psi = 0.207\lambda + 0.062\lambda^2 \tag{18}$$

$$\lambda = 6.441Z/(1 + 6.441Z) \tag{19}$$

$$\alpha = 0.933(4Z/0.6)^{0.092} \tag{20}$$

Although such behavior has been established experimentally in poor solvents by varying temperature and M,[11] Fujita[28] has recently questioned the decrease of Ψ in good solvents when α is decreased toward unity as the chain length is shortened. Some support for this exists since for very low molecular weight PS in toluene the SANS data of Huber et al.[29] in fact show the opposite trend to that in Figure 11; i.e., Ψ increases sharply as α goes to unity, a finding which is most probably related to changes in chain stiffness.[30]

Dynamical Properties. Intrinsic Viscosity–Coil Expansion. Figure 12 gives experimental data for the viscosity expansion factor

$$\alpha_\eta = ([\eta]/[\eta]_\Theta)^{1/3} \tag{21}$$

where $[\eta]$ refers to data in $CHCl_3$ (25 °C) and $[\eta]_\Theta$ to benzene (24.5 °C). The continuous line in Figure 12, which agrees well with the experimental data, is that given in terms of the expansion parameter $\bar{z}$ by the RG theory[5] with no adjustable parameters and assumption of non-draining character

$$\alpha_\eta^3 = (1 + (32\bar{z}/3))^{3/8}\{1 - 0.276[((32\bar{z}/3))/(1 + (32\bar{z}/3))]\} \tag{22}$$

for $\bar{z} < 0.15$ and

$$\alpha_\eta^3 = 2.02\bar{z}^{0.5508} \tag{23}$$

for $\bar{z} > 0.75$ where

$$\bar{z} = 0.906[(T - \Theta)/T]M^{1/2} \tag{24}$$

where T is the absolute temperature and Θ the theta temperature. The close agreement observed here between theory and experiment is surprising in view of the partial draining character suggested by the ratio $\rho = R_g/R_h$.

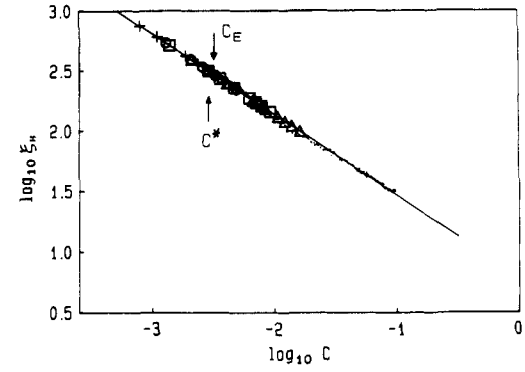

Figure 13. Log–log plot of the dynamic correlation length vs concentration for the PIB/$CHCl_3$ system at 25 °C. The slope is -0.67_5. The values of C^* and C_E which are included refer to $M = 3.8 \times 10^6$ (small dots). Lower molecular weights are 1.82×10^5 (○), 2.47×10^5 (△), 6.1×10^5 (□), and 1.1×10^6 (+).

Dynamic Correlation Length—Semidilute Solutions of PIB. The dynamic correlation length was evaluated from the cooperative diffusion coefficient (D_C) in chloroform by using the relationship

$$\xi_h = kT/6\pi\eta_0 D_C \tag{25}$$

with $D_C = \Gamma/q^2(1 - \Phi)$; q is the scattering vector and the factor $(1 - \Phi)$ corrects for solvent backflow. This quantity is shown as a function of the concentration in a log–log diagram in Figure 13. The slope, which has been precisely determined by about 50 data points assembled on a PIB fraction with $M = 3.8 \times 10^6$, is -0.67_5, a value which is typical for that found for polystyrenes in a number of good solvents.[6] We also observe that the ξ values for PIB superimpose exactly on those recently collected[6] for a large number of similar data for polystyrene in good solvents over a similar interval in concentration.

A plot of these data in terms of the reduced variables used in RG theory is shown in Figure 14. On the vertical axis (ξ_h/R_h) is plotted vs the universal parameter X, and the result is compared with the theoretical curve proposed by Shiwa,[26] taking into account hydrodynamic screening. In the case of the experimental data, X has been put equal to $0.87k_DC$.[27] Whereas precise agreement with theoretical prediction is observed for polystyrene, in the case of PIB a small deviation is noted. The agreement is gratifying, however, considering the wide range of concentration used (up to about $C/C^* = 30$) and also that RG treatments for the dynamic properties do not take into account the effect of topological constraints and are also unable to describe the effect of partial draining characteristics. The entanglement properties of PS and the relatively flexible PIB differ substantially. Thus, for example, the entanglement concentration (C_E; refs 31, 32) for a fraction of $M = 5 \times 10^6$ is 0.43% for PS and 0.24% for PIB.

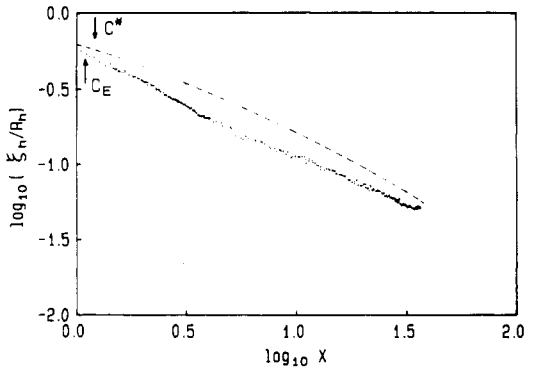

Figure 14. Plots of the reduced dynamic correlation length vs the universal parameter X according to renormalization group theory. The experimental points are plotted with $X = 0.87k_DC$, and the dashed theory line is given according to the ıression of Shiwa,[26] taking into account hydrodynamic screeı.....ₚ. All of the data are in the entangled regime for a fraction of $M = 3.8 \times 10^6$ in chloroform at 25 °C.

Conclusions. It is concluded that the solution properties of PIB are remarkably similar to those of polystyrene in good solvents in both dilute and semidilute regimes. The differences that are apparent in dilute solution, for example, in draining character, are not more pronounced than the variation observed for PS itself in different thermodynamically good solvents. As might be anticipated, the influence of backbone structure is not perceived in semidilute solution even though PIB is much more flexible than PS, since the topological constraints, giving rise to temporary entanglements, should be small when the thermodynamic interactions are strong. In intermediate and poor solvent qualities this will not be so, however. Universal behavior is observed in the scaling plots over extended ranges of concentration. Qualitatively and quantitatively similar systematic deviations from the predicted behavior of renormalization group theory are apparent with regard to the osmotic compressibility. For both types of chain there is a close correspondence between the predictions of theory and the experimental data with regard to dynamical behavior in semidilute solution.

Acknowledgment. Financial support from the Swedish Natural Science Research Council (NFR) and the Swedish Board for Technical Development (STU) is gratefully acknowledged.

References and Notes

(1) Zhou, P.; Brown, W. *Macromolecules* **1989**, *22*, 890.
(2) Brown, W.; Zhou, P. *Macromolecules* **1989**, *22*, 4031.
(3) Brown, W.; Zhou, P. *Polymer* **1990**, *31*, 772.
(4) Brown, W.; Zhou, P. *Macromolecules* **1991**, *24*, 1820.
(5) Freed, K. F. *Renormalization group theory of macromolecules*; Wiley: New York, 1987.
(6) Brown, W.; Nicolai, T. *Colloid Polym. Sci.* **1990**, *268*, 977.
(7) Pike, E. R.; Pomeroy, W. R. M.; Vaughan, J. M. *J. Chem. Phys.* **1975**, *62*, 3188.
(8) Nicolai, T.; Brown, W.; Johnsen, R. M.; Stepanek, P. *Macromolecules* **1990**, *23*, 1165.
(9) Jakes, J., to be published.
(10) Brown, W.; Stilbs, P. *Polymer* **1982**, *23*, 1780.
(11) Yamakawa, H. *Modern Theory of Polymer Solutions*; Harper and Row: New York, 1971.
(12) Brown, W.; Mortensen, K. *Macromolecules* **1988**, *21*, 420.
(13) Oono, Y.; Kohomoto, M. *J. Chem. Phys.* **1983**, *78* (1), 520.
(14) Schmidt, M.; Burchard, W. *Macromolecules* **1981**, *14*, 210.
(15) Zimm, B. H. *Macromolecules* **1980**, *13*, 592.
(16) Miyaki, Y.; Einaga, Y.; Fujita, H. *Macromolecules* **1978**, *11*, 1180.
(17) Appelt, B.; Meyerhoff, G. *Macromolecules* **1980**, *13*, 657.
(18) Bhatt, M.; Jamieson, A. M. *Macromolecules* **1988**, *21*, 3015.
(19) Douglas, J. F.; Freed, K. F. *Macromolecules* **1984**, *17*, 2344.
(20) Nemoto, N.; Makita, Y.; Tsunashima, Y.; Kurata, M. *Macromolecules* **1984**, *17*, 425.
(21) Ohta, T.; Oona, Y. *Phys. Lett.* **1982**, *89A*, 460.
(22) Oona, Y.; Baldwin, P. R.; Ohta, T. *Phys. Rev. Lett.* **1984**, *53*, 2149.
(23) Wiltzius, P.; Haller, H. R.; Cannell, D. S.; Schaefer, D. W. *Phys. Rev. Lett.* **1983**, *51*, 1183.
(24) Zhou, P.; Brown, W. *Macromolecules* **1990**, *23*, 1131.
(25) Oona, Y.; Freed, K. F. *J. Phys. A: Math. Gen.* **1982**, *15*, 1931.
(26) Shiwa, Y. *Phys. Rev. Lett.* **1987**, *58*, 2102.
(27) Nyström, B.; Roots, J. *J. Polym. Sci. C: Polym. Lett.* **1990**, *28*, 101.
(28) Fujita, H. *Macromolecules* **1988**, *21*, 179.
(29) Huber, K.; Bantle, S.; Lutz, P.; Burchard, W. *Macromolecules* **1985**, *18*, 1461.
(30) Huber, K.; Stockmayer, W. H. *Macromolecules* **1987**, *20*, 1400.
(31) $C_E = \rho M_E/M$, where $\rho = 1.39$; M_E (8600) is the entanglement molecular weight for PIB[32] and M the molecular weight of polymer.
(32) Ferry, J. D. *Viscoelastic Properties of Polymers*; Wiley: New York, 1980.
(33) Akcasu, A. Z. *Polymer* **1981**, *22*, 1169.
(34) Tsunashima, Y.; Hirata, M.; Nemoto, N.; Kurata, M. *Macromolecules* **1987**, *20*, 1992, 2862; **1988**, *21*, 1107.
(35) Nemoto, N.; Makita, Y.; Tsunashima, Y.; Kurata, M. *Macromolecules* **1984**, *17*, 425.
(36) Miyaki, Y.; Einaga, Y.; Fujita, H. *Macromolecules* **1978**, *11*, 1180.
(37) Akcasu, A. Z.; Benmouna, M.; Alkhafaji, S. *Macromolecules* **1981**, *14*, 147.
(38) (a) Kubota, K.; Fujishige, S.; Ando, I. *Polym. J.* **1990**, *22*, 15. (b) Kubota, K.; Hamano, K.; Kuwahara, N.; Fujishige, S.; Ando, I. *Polym. J.* **1990**, *22*, 1051.

Registry No. PIB (homopolymer), 9003-27-4.